

Relation between the Peak Acceleration of Aortic Blood Flow and End-diastolic Aortic Pressure in Intact Dogs

Byoung G. Min and Hee C. Kim

Department of Biomedical Engineering, College of Medicine, Seoul National University, Seoul 110, Korea

Abstract—A quantitative analysis based upon the equivalent circuit model of the left ventricle-systemic circulation was performed to study the afterload dependency of the peak acceleration of the left ventricular ejection flow. Also, in experiments with conscious dogs, the left ventricular pressure, the left ventricular minor axis dimension, and the aortic flow were measured using implanted transducers before and after quick inflation of a pneumatic occluder (balloon), circumferentially placed in the descending aorta, to induce changes of the peripheral impedance with a constant ventricular contractile state and preload. The present circuit analysis shows that the peak acceleration at the onset of the impulse-like pressure source is dependent upon the factors of the ventricular performance, and also on peripheral conditions. The present animal experiments in unanesthetized dogs confirmed the above theoretical results by showing significant changes of the peak acceleration of aortic flow after changes of the peripheral impedances. ($1052 \pm 431(\text{cc/sec}^2)$, $p < 0.001$ during aortic occlusion and $-1833 \pm 799(\text{cc/sec}^2)$, $p < 0.001$ during aortic release) Also, as suggested in the analysis, the high negative correlation coefficients (-0.74 , $p < 0.01$ during aortic occlusion and -0.83 , $p < 0.01$ during aortic release) between the peak acceleration and the end diastolic arterial pressure were shown in the animal experiments. The present study shows that the peak acceleration of the left ventricular blood flow may be used as an index of the left ventricular performance, only when one compares the ventricular function at constant input impedance condition.

Key words: *Peak acceleration, Aortic blood flow, End-diastolic aortic pressure*

INTRODUCTION

Rushmer suggested that the ventricle acts as an impulse generator and the "initial ventricular impulse" can be used as a useful index of myocardial performance (Rushmer *et al.* 1964). This view was further supported by Noble *et al.* (1966) from the observation of the high sensitivity of the maximum acceleration of the blood flow in the early ejection phase to the intracoronary injection of stimulating drugs, prior to any changes in stroke volume. Based upon these observations, the peak acceleration of the blood flow in the ascending aorta was proposed as an index of the contractile state of the left ventricle.

On the other hand, Wilcken and his coinvestigators observed that the peak acceleration was changed with the alteration in aortic impedance

(Wilcken *et al.* 1964). In this case, the peak acceleration cannot represent the intrinsic left ventricular contractile state. To evaluate the above conflicting results, we studied quantitatively the hemodynamic factors influencing the peak acceleration of aortic flow using the equivalent circuit analysis of the left ventricle-systemic circulation model. Also, we performed animal experiments in conscious dogs to validate our analysis.

MATERIALS AND METHODS

1. Analysis

To evaluate quantitatively the changes of the peak acceleration in response to the changes of aortic input impedance, we have used the equivalent circuit analysis on the left ventricle-systemic circulation model of other investigators (Abel *et al.* 1966, 1971; Buoncrisiani *et al.* 1973; Elzinga *et al.*

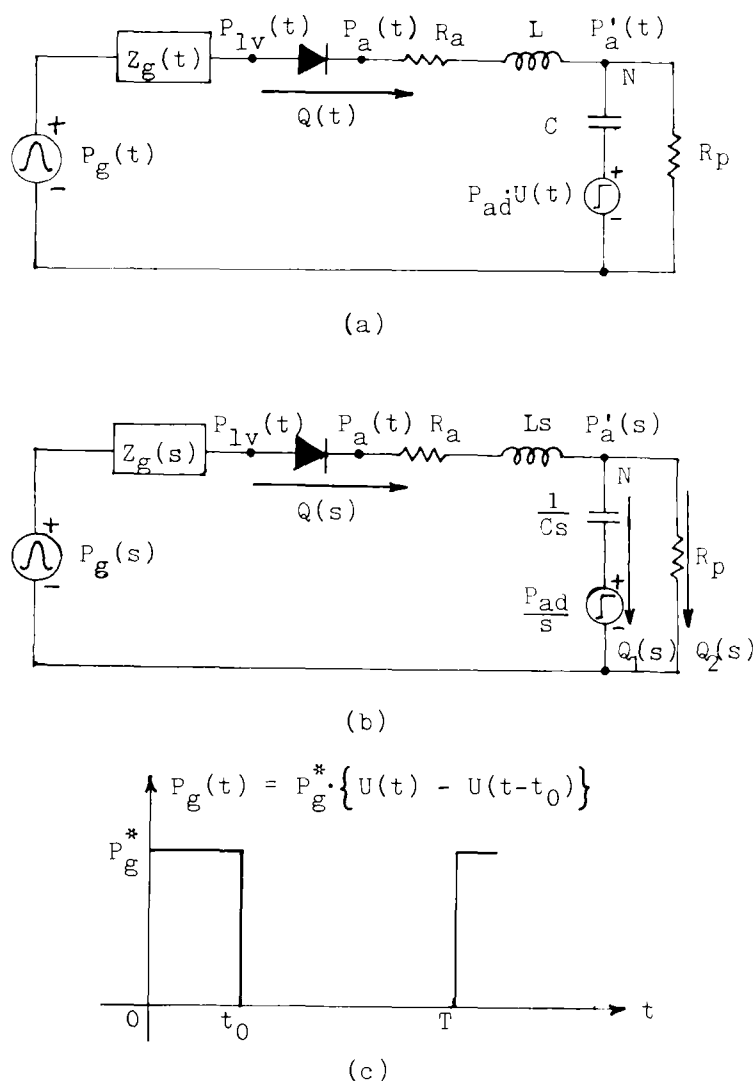


Fig. 1. (a) The equivalent circuit model of the ventricle-systemic circulatory system. (b) The circuit model represented by Laplace transform with initial conditions. (c) Waveforms of source pressure, $P_g(t)$.

1973, 1974, 1976; Westerhof *et al.* 1973). In theoretical analysis, the left ventricle is considered to consist of a voltage source (P_g) and a series source impedance (Z_g) in Fig. 1. The afterload of the left ventricle is simulated in the model as a combination of a diode of aortic valve in series with an inductance (L), and a resistance (R_a), representing characteristic aortic impedance. For the peripheral circulation, the arterial capacitance (C) is connected in parallel with a peripheral resistance (R_p) as shown in Fig. 1. In the model, the voltage is equivalent to the pressure components, and the current represents the blood flow. (refer APPENDIX).

2. Animal experiments

To study the afterload dependency of the peak acceleration in conscious dogs, we performed the

following experiment. The experimental protocol was similar to Noble *et al.*'s (1966) and Wilcken *et al.*'s (1964) except that the present measurements were performed in the conscious unanesthetized dogs.

On the first day of experiment, the measuring transducers were implanted in mongrel dog after anesthesia. An electromagnetic flow probe (HONEYWELL) was fitted around the root of the ascending aorta, and a latex balloon was looped around the descending aorta. This balloon was used to produce a partial aortic occlusion after balloon inflation. Pacing electrodes were attached to the right atrium to control the heart rate and maintain it constant during the experiment. A catheter-tip pressure transducer (Millar MIKRO-TIP[®]) was located in the left ventricle or aortic root for measurement of L.V. or aortic pressure. Ultrasonic transducers for a sonocardiometer were implanted on the endocardium of the left ventricle, through puncture wounds, to measure the L.V. minor axis dimension, a sensitive measure of a change in L.V. volume. Ten days after the above transducers implantation, the experiment was performed in the conscious state without anesthesia, and this data were used for analysis. For the present study, this surgical procedure was performed on eight mongrel dogs (14 to 19 Kg). Two of them died during the study, and in another case, we failed to place the balloon occluder properly. The experimental results were taken from the remaining five dogs. To discriminate the effects of the time interval of the balloon occlusion, the experiments were performed with broad spectrum of occlusion time intervals (30 msec to 2 min).

3. Measurements and data processing

Fig. 2(a) and (b) show a sample waveforms of aortic pressure, the acceleration, aortic flow, and the L.V. dimension before and after balloon inflation and deflation, respectively. Aortic flow signal was used as an input to an electronic derivative circuit for measuring the peak acceleration of aortic flow. A four channel paper recorder was used to recording of L.V. pressure, or aortic pressure, the aortic flow, the acceleration of aortic flow, and the L.V. dimension. A Houston Instrument HI-PAD[™] digitizer was used to digitize the paper recorded data as the input to a IBM-PC/XT computer for further analysis. The ejection phase was selected using the points where aortic flow crossed the zero level. Then, the two points on the L.V., or aortic pressure waveform corresponding to the onset and

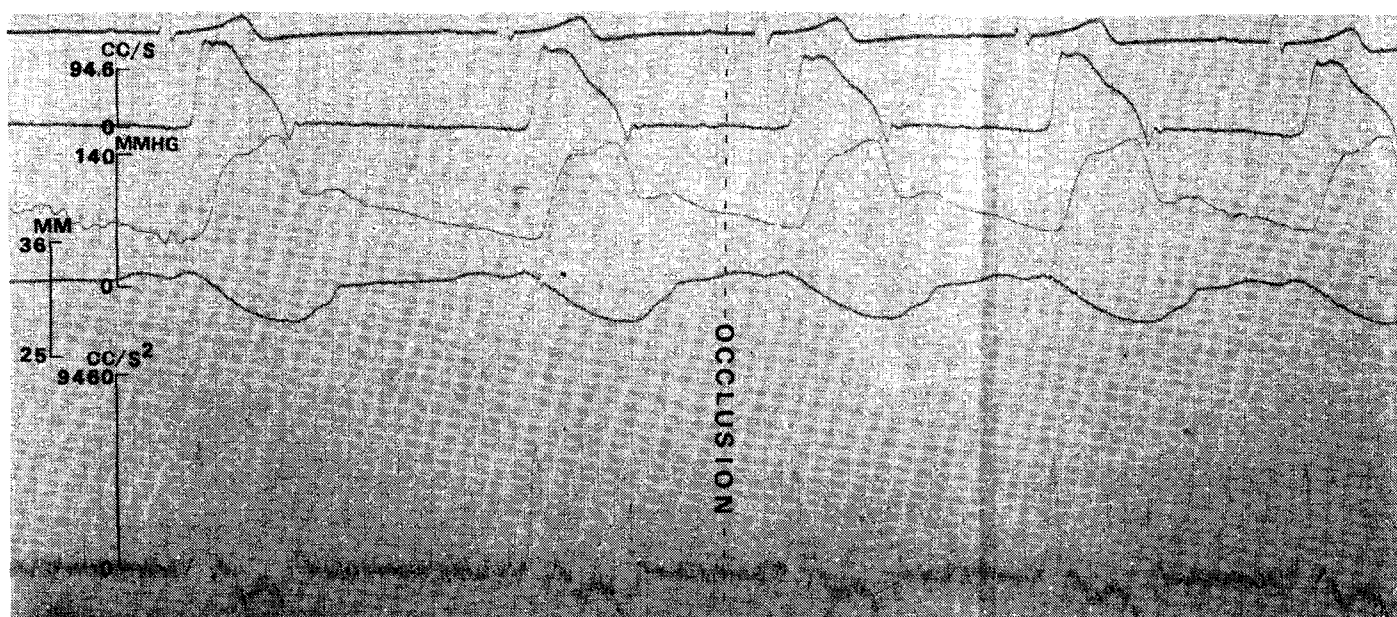


Fig. 2-(a)

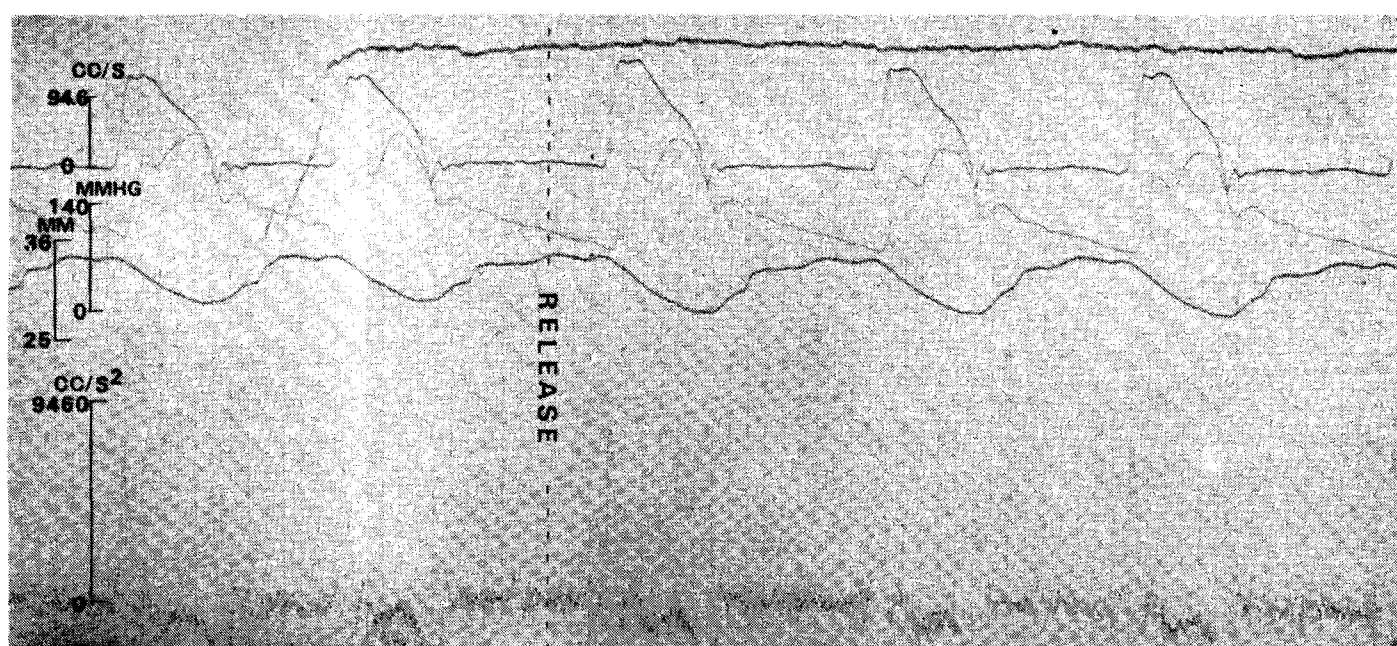


Fig. 2-(b)

Fig. 2. (a) Waveforms of aortic flow (second), aortic pressure (third), LV minor axis (fourth), and the acceleration of aortic flow (bottom) before and after partial aortic occlusion. (b) Same waveforms before and after release of partial aortic occlusion.

the ending of the ejection phase were used as the arterial end-diastolic pressure (P_{ad}) and the arterial end-systolic pressure (P_{as}), respectively. Source pressure, P_g , was estimated using Fast Fourier Series from the two adjacent beats using the data of L.V. pressure and aortic flow (Min *et al.* 1976). The values of peak acceleration, P_{ad} , left ventricular stroke dimension, ejection time, and end-diastolic L.V. minor axis were measured through-

out the balloon inflation and deflation procedures. A correlation coefficient between the peak acceleration and P_{ad} was also calculated.

RESULTS

The changes of peak acceleration was shown to be sensitive to the changes of input impedance produced by the balloon occlusion and release. Fig. 3 and 4 show noticeable changes of peak

acceleration after the balloon occlusion and release, respectively. While there were clear changes in peak acceleration, we could not observe any significant changes of LV stroke dimension as shown in Fig. 5 and 6. Also, the LV ejection time and the end-diastolic LV minor axis diameter, which are related to the contractile state of LV and the preload did not change during the balloon operation as shown in Fig. 7, 8, 9, 10.

The end-diastolic arterial pressure are shown to be sensitively changed following the balloon inflation and deflation in Fig. 11 and 12. These changes are inversely related to those of the peak acceleration. It should be noted that there exists an almost linear relationship with negative slopes between peak acceleration and P_{ad} as shown in Fig. 13 and 14. These relations are implied in our present analytical results.

The estimated LV source pressures, P_g , are shown in Fig. 15. It shows that there exists some increase of source pressure between the initial and final time of balloon occlusion, when this duration is long.

DISCUSSION

The results of the present study were basically similar to the experimental results reported by Wilcken *et al.* (1964). The peak acceleration diminished by $1054 \pm 431 (\text{cc/sec}^2)$ after aortic occlusion and it increased by $1833 \pm 799 (\text{cc/sec}^2)$ after release of the aortic occlusion. We could also observe that the elevation of the peak acceleration after balloon deflation was much greater than its diminution after balloon inflation in dogs with longer occlusion period (longer than one minute). This result was also consistent with other investigators' observations (Wilcken *et al.* 1964).

Theoretical analysis and animal experiments in the conscious dogs with chronically implanted transducers were performed to study the factors influencing the peak acceleration of left ventricular blood flow. as a result of circuit analysis of Eq. (8), the peak acceleration is shown to be related to the difference between the source pressure and the end-diastolic arterial pressure, P_{ad} . The experimental data also validates this analytical result with high correlation coefficients (-0.74 and -0.83 for balloon inflation and deflation, respectively, $p < 0.01$) between the peak acceleration and the end-diastolic pressure.

In the second-order mechanical system consisting of a mass (M) only, the applying force (F) is related to the acceleration of the mass by Newton's

law; $F = MA$. This relationship can be expressed in terms of electrical circuit elements in direct analogue form by the equation;

Since Noble *et al.* (1966) assumed that at the time of maximum acceleration, only the inertance component dominates the opposition to left ventricular ejection, the peak acceleration of flow was shown to be directly related to the afterload independent cardiac force, which can be represented by P_g^*/L in the present circuit analysis.

However, the left ventricle and its peripheral circulatory system can be more accurately represented by a force generator (pressure source) with the source impedance. And, they are connected to the combined loads of mass (inertia), resistance component, and the elastic components.

The present analysis shows that the peak acceleration at the onset of the impulse-like pressure source is dependent upon the factors including source and peripheral impedances. In our present study and other investigators' experimental study, the peak acceleration was affected by the alteration of input impedance. Especially, in our circuit analysis, P_{ad} was shown to be an important parameter, where P_{ad} was affected by the changes of the peripheral resistance and the arterial capacitance in addition to the source parameters. Changes of the input impedance can alter the time constant of arterial pressure waveform during diastolic phase and the end-systolic arterial pressure P_{as} , which, in turn, is related to the alteration of P_{ad} . The present experiments confirmed the above theoretical results by showing a high correlation coefficient between the parameters (peak acceleration and P_{ad}) in the range of from -0.6 to -0.9 . In the present study, we have assumed that the source pressure acts as an impulse with finite duration, and thus, the peak acceleration occurs at the onset of ejection. These are based upon Rushmer's conclusion (Rushmer *et al.* 1964, 1962) other authors' observations (Noble *et al.* 1966; Wilcken *et al.* 1964; Sonnenbick *et al.* 1962, 1962).

Another assumption of the present study is that, for two or three beats just after aortic occlusion or release of occlusion, the ventricular contractility and the preload have not changed. This assumption is based on the present observations of no significant changes in ventricular dimensional waveform in two beats, and, also, of other investigators' observations (Noble *et al.* 1966; Min *et al.* 1976; Levine *et al.* 1964; Noble *et al.* 1964) suggesting that changes in impedances between two consecutive beats do not result in variation in the

contractile state. From the above results, we may conclude that the changes of the peak acceleration just after the changes of the impedance condition are not caused by changes of the source pressure but due to the variation in the input impedance.

As shown in Fig. 15, the computed source pressure, representing the contractile state of the ventricle has increased, when the partial occlusion state continued for longer than one minute. These differences in hemodynamic parameters and its changes after the balloon inflation and deflation in the group of the longer occlusion period may be mainly due to the difference of the source pressure between the two states.

Based upon the above results, the peak acceleration of left ventricular blood flow may be used as an index of the left ventricular contractile state, only when we compare the ventricular functions at the constant input impedance conditions. In the case of the altered arterial system, the peak acceleration may not be a reliable index of left ventricular contractile performance.

APPENDIX

The present analysis is restricted to the ejection phase where the aortic valve opens at $t=0$, and it is assumed that the ventricular pressure, $P_v(t)$, equals aortic root pressure, $P_a(t)$, at all times when the aortic valve is open. In Figure 1, the aortic flow during ejection phase is related to the source parameter and the vascular input impedance, as well as the arterial end-diastolic pressure, acting as the capacitance's initial stored voltage. Thus, in circuit analysis, P_{ad} is replaced by an initial condition generator, $P_{ad} \cdot U(t)$, as shown in Fig. 1(a).

Applying Kirchhoff's current law at the node N for the ejection period, the Laplace transform of aortic flow, $Q(s)$, becomes

$$\begin{aligned} Q(s) &= Q_1(s) + Q_2(s) \\ &= Cs \left\{ P'_a(s) - \frac{P_{ad}}{s} \right\} + \frac{1}{R_p} P'_a(s). \end{aligned} \quad (1)-a$$

or directly,

$$Q(s) = \frac{P_g(s) - P'_a(s)}{Z_g(s) + R_a + Ls} \quad (1)-b$$

where P'_a is the pressure at the node N, and (s) represents the Laplace transform. Equalizing the right sides of Eqs. (1)-a and (1)-b, it is given by

$$P'_a(s) = \frac{P_g(s) + (Z_g(s) + R_a + Ls) \cdot C \cdot P_{ad}}{(Z_g(s) + R_a + Ls)(Cs + 1/R_p) + 1} \quad (2)$$

Eliminating $P'_a(s)$ from Eq.(1)-b using Eq.(2), the ejection flow transform, $Q(s)$, can be related as follows;

$$\begin{aligned} &\left\{ 1 + (Cs + \frac{1}{R_p}) \cdot (Z_g(s) + R_a + Ls) \right\} \cdot Q(s) \\ &= (Cs + \frac{1}{R_p}) \cdot P_g(s) - C \cdot P_{ad} \end{aligned} \quad (3)$$

Representing source pressure $P_g(t)$ as an impulse with finite duration as shown in Fig. 1(c), based upon Rushmer's observation (Rushmer *et al.* 1964) that the pumping action of the ventricles can be represented in terms of initial impulse, defined as the product of force and time, we can assume for the analysis that the maximum acceleration occurs at the early onset phase of ejection close to the instant of $t=0^+$.

This analysis is also related to the report (Rushmer *et al.* 1964) that the maximum rate of myocardial shortening occurs at the onset of contraction so that initial velocity is the greatest during contraction. Then, using the properties of the Laplace transform, related to the differentiation with respect to time and the initial-value property, the peak acceleration can be obtained as follow;

$$\begin{aligned} \frac{dQ(t)}{dt} \Big|_{\max} &= \frac{dQ(t)}{dt} \Big|_{t=0^+} \leftrightarrow \lim_{s \rightarrow \infty} s \\ &\cdot \{sQ(s)\}, \end{aligned} \quad (4)$$

and from Eq.(3),

$$\begin{aligned} \lim_{s \rightarrow \infty} s \cdot \{sQ(s)\} &= \\ &\lim_{s \rightarrow \infty} \frac{s^2 \{ (Cs + 1/R_p) \cdot P_g(s) - CP_{ad} \}}{(Cs + 1/R_p) \cdot (Z_g(s) + R_a + Ls) + 1} \end{aligned}$$

where " \leftrightarrow " represents a Laplace transform pair.

At the infinite limit of the right side of Eq.(4), the lower power terms of " s " can be deleted, and the result becomes;

$$\frac{dQ(t)}{dt} \Big|_{\max} \leftrightarrow \lim_{s \rightarrow \infty} \frac{s^2 \cdot P_g(s) + sP_g(s)/R_p C - P_{ad}s}{Ls + Z_g(s)} \quad (5)$$

For the source impedance, $Z_g(s)$, as it consists of passive lumped-elements, the degree of its numerator polynomial may be the same as the degree of the denominator polynomial, or they can be different only by unity (Brenner 1967). Then, the limit value of $Z_g(s)$ becomes;

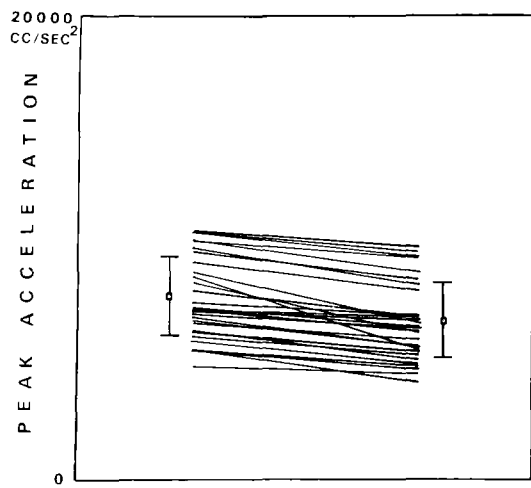


Fig. 3. Changes of the peak acceleration after aortic occlusion; mean and standard deviation of difference between pre- and post- occlusion = 1052 ± 431 (cc/sec²) ($P < 0.001$)

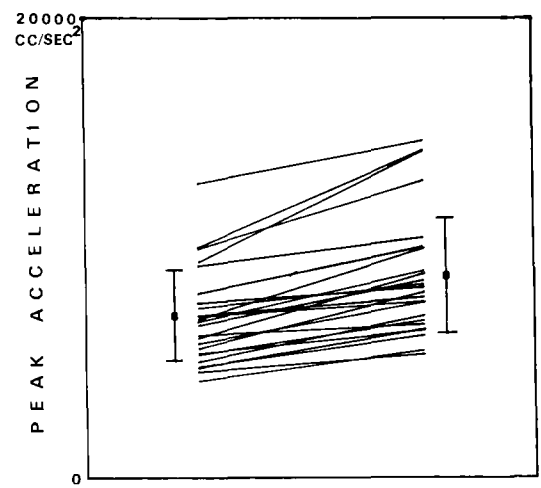


Fig. 4. Changes of the peak acceleration after release of aortic occlusion; mean and standard deviation of difference between pre- and post- release = -1883 ± 799 (cc/sec²) ($P < 0.001$)

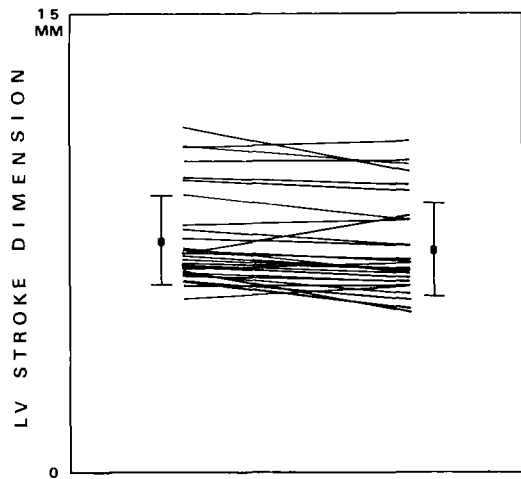


Fig. 5. Changes of the LV stroke dimension after aortic occlusion; mean and standard deviation of difference between pre- and post- occlusion = 0.32 ± 0.37 (mm) ($P < 0.01$)

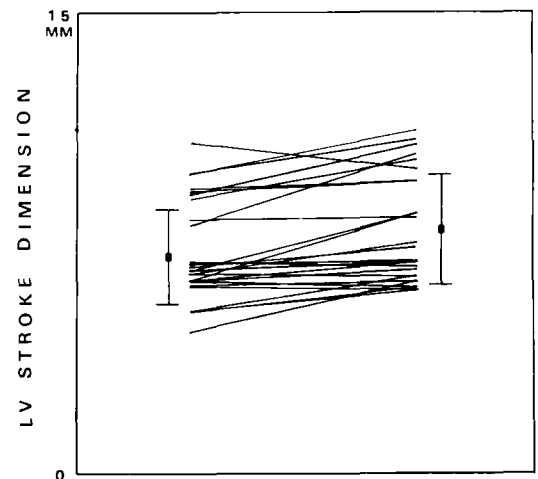


Fig. 6. Changes of the LV stroke dimension after release of aortic occlusion; mean and standard deviation of difference between pre- and post- release = -0.70 ± 0.58 (mm) ($P < 0.001$)

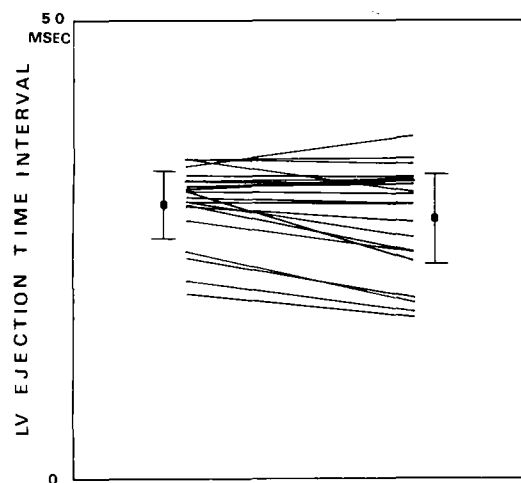


Fig. 7. Changes of the LV ejection time interval after aortic occlusion; mean and standard deviation of difference between pre- and post- occlusion = 1.30 ± 1.66 (msec) ($P < 0.01$)

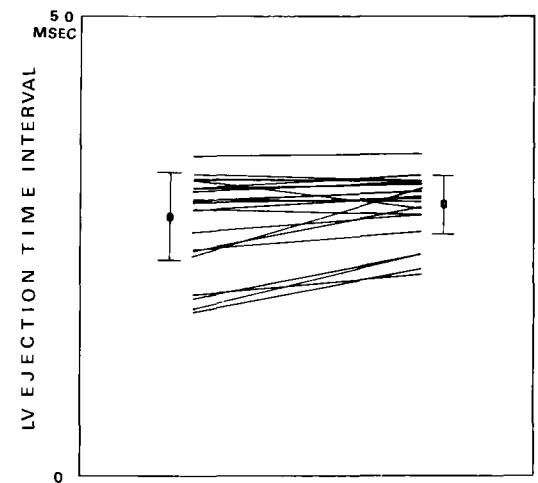


Fig. 8. Changes of the LV ejection time interval after release of aortic occlusion; mean and standard deviation of difference between pre- and post- release = 1.41 ± 1.70 (msec) ($P < 0.01$)

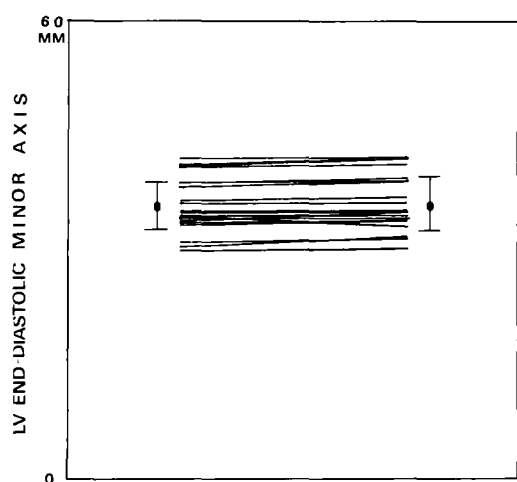


Fig. 9. Changes of the LV end-diastolic minor axis diameter after aortic occlusion; mean and standard deviation of difference between pre- and post-occlusion = -0.22 ± 0.32 (mm) ($P < 0.25$)

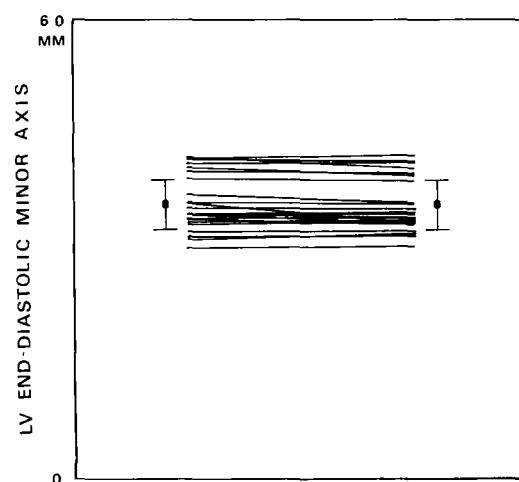


Fig. 10. Changes of the LV end-diastolic minor axis diameter after release of aortic occlusion; mean and standard deviation of difference between pre- and post- release = 0.33 ± 0.48 (mm) ($P < 0.25$)

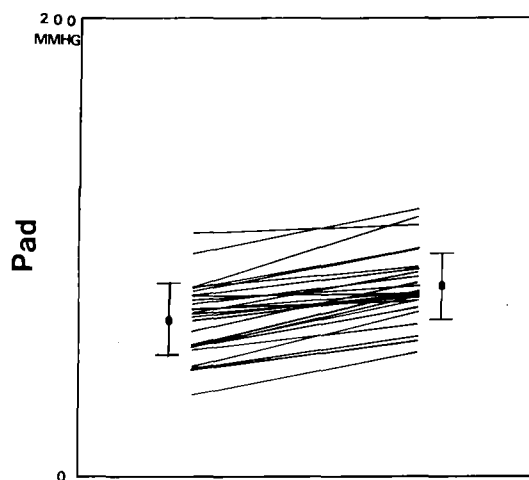


Fig. 11. Changes of the end-diastolic arterial pressure (Pad) after aortic occlusion; mean and standard deviation of difference between pre- and post-occlusion = -16.34 ± 5.0 (mmHg) ($P < 0.001$)

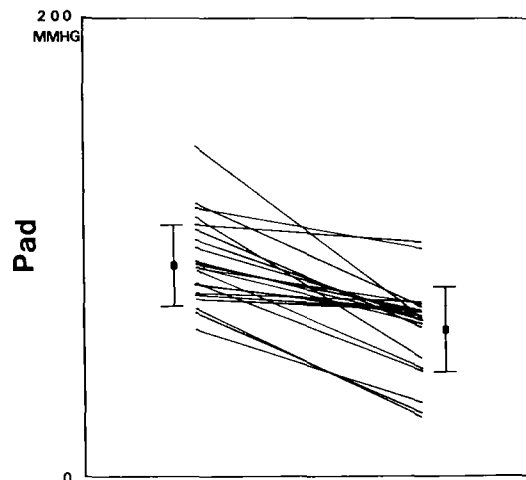


Fig. 12. Changes of the end-diastolic arterial pressure (Pad) after release of aortic occlusion; mean and standard deviation of difference between pre- and release = 27.56 ± 14.46 (mmHg) ($P < 0.001$) occlusion = 1052 ± 431 (cc/sec) ($P < 0.001$)

$$\lim_{s \rightarrow \infty} Z_g(s) = \begin{cases} \text{constant including zero,} \\ \text{when degree of numerator} \geq \text{degree of denominator.} \\ Z_g^* s, \\ \text{when degree of numerator} < \text{degree of denominator, and } Z_g^* \text{ is constant.} \end{cases} \quad (6)$$

From Fig. 1(c), the Laplace transform of source pressure, $P_g(t)$, can be represented as,

$$P_g(s) = \frac{P_g^*}{s} (1 - \exp(-st_0)), \quad (7)$$

where P_g^* is constant.

From Eqs.(6) and (7), the peak acceleration can be described as follows;

$$\left. \frac{dQ(t)}{dt} \right|_{\max. \text{ at } t=0^+} = \begin{cases} \frac{P_g^* - P_{ad}}{L}, & \text{when } \lim_{s \rightarrow \infty} Z_g(s) = \text{constant.} \\ \frac{P_g^* - P_{ad}}{L + Z_g^*}, & \text{when } \lim_{s \rightarrow \infty} Z_g(s) = Z_g^* \cdot s. \end{cases} \quad (8)$$

The final result of Eq.(8) shows that the arterial end-diastolic pressure, P_{ad} , as well as P_g^* can affect the peak acceleration for the constant values of L and Z_g^* during ejection phase.

Then, we have studied the factors influencing P_{ad} . When the aortic valve is closed, the peripheral

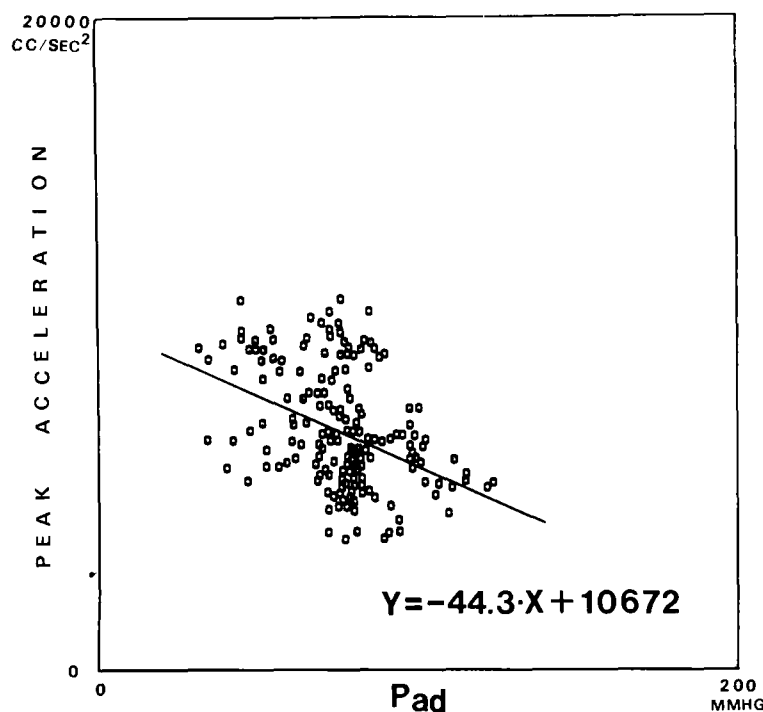


Fig. 13. Relationship between the peak acceleration and the end-diastolic arterial pressure (Pad) including all data of pre- and post- occlusion; average of the correlation coefficients = -0.74 ($P < 0.01$)

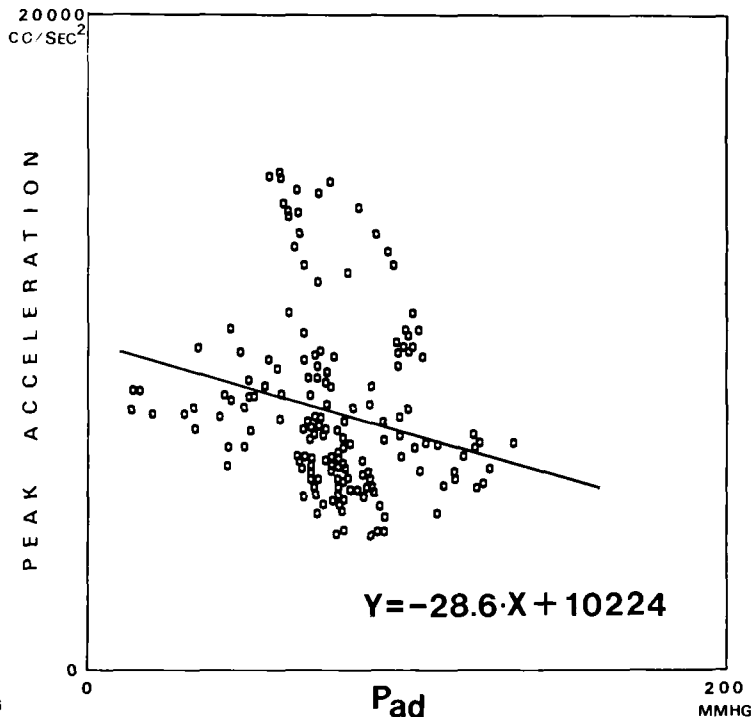


Fig. 14. Relationship between the peak acceleration and the end-diastolic arterial pressure (Pad) including all data of pre- and post- release; average of the correlation coefficients = -0.83 ($P < 0.01$)

pressure, $Pa'(t)$, is equal to the aortic root pressure, $Pa(t)$, and it decreases exponentially from the aortic (or arterial) pressure at the valve closing time, Pa_s , down to Pad with a time constant of R_pC during the diastolic phase in Figure 1(a). Thus, the arterial end-diastolic pressure is determined by the properties of the arterial tree (time constant, R_pC), the factor related to the preceding beat (Pa_s), and the diastolic time duration ($T-t_0$).

Using the voltage division rule in Figure 1(b), the transform of the arterial pressure, $Pa'(t)$, before and after valve closing time $t=t_0$, can be represented as follows;

$$Pa'(s) = \frac{1}{(1/R_p + Cs)} \cdot P_g(s) \cdot \frac{1}{(Z_g(s) + R_a + Ls) + \left(\frac{1}{1/R_p + Cs}\right)}$$

$$= \frac{R_p}{R_p + (1 + R_pCs)(Z_g(s) + R_a + Ls)} \cdot P_g(s) \quad (9)$$

for $0^+ < t < t_0$, and

$$Pa'(s) = \frac{\exp(-st_0)}{s + R_pC} \cdot Pa_s, \text{ or}$$

$$Pa'(t) = Pa_s \cdot \exp \left[- (t-t_0)/R_pC \right] \quad (10)$$

for $t_0 < t < T$.

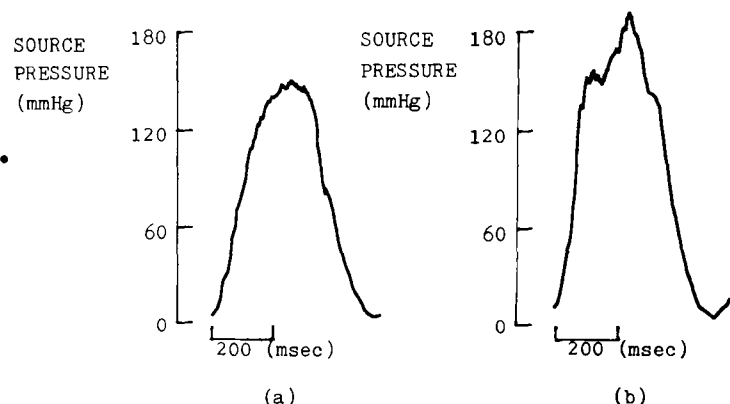


Fig. 15. Computed source pressure in control state (a); and after two minute of continuous aortic occlusion (b).

Eq.(9) can be simplified to Eq.(11) using an approximation of the term $(1 + R_pCs)$ to unity for typical values of R_p and C .

$$Pa'(s) = \frac{R_p}{R_p + (Z_g(s) + R_a + Ls)} \cdot P_g(s) \quad (11)$$

for $0^+ < t < t_0$.

For the two consecutive beats before and after aortic occlusion, we can expect that with constant $P_g(s)$ and $(Z_g(s) + R_a + Ls)$, and with the increase of peripheral resistance R_p , each harmonics of $Pa'(t)$ increases parabolically to these of $P_g(t)$. The above analysis shows that aortic pressure at the

time of valve closing, P_{as} , increases up to the level of the source pressure P_g at the time of $t=t_0$ with an increase of R_p .

As a result of circuit analysis, we can conclude that, for the same P_g , the peak acceleration of ejected blood changes as a function of the arterial end-diastolic pressure, P_{ad} . On the other hand, P_{ad} is determined by P_{as} , the time constant ($R_p C$), and the diastolic period. Also, it is shown that the end-systolic arterial pressure, P_{as} , represents a portion of the source pressure, P_g , with its magnitude varies depending upon the ratio of the peripheral resistance to the sum of the source and characteristic impedances.

REFERENCES

- Abel FL.** An analysis of left ventricle as a pressure and flow generator in the intact systemic circulation. *IEEE Trans. Biomed. Eng.* 1966, 13:182-188
- Abel FL.** Fourier analysis of left ventricular performance. *Circulation Res.* 1971, 28:119-135
- Brenner E, Javid M.** Analysis of electric circuit. McGraw-Hill Inc. 1967, 2ed.:273
- Buonocristiani JF, Liedtke AJ, Stong RM, Urschel CW.** Parameter estimates of a left ventricular model during ejection. *IEEE Trans. Biomed. Eng.* 1973, 20:110-114
- Elzinga G, Westerhof N.** Pressure and flow generated by the left ventricle against different impedances. *Circulation Res.* 1973, 32:178-186
- Elzinga G, Westerhof N.** End-diastolic volume and source impedance of the heart. In the physiological basis of Starling's law of the heart. Ciba Foundation Symposium 1974, 24:251-255
- Elzinga G, Westerhof N.** The pumping ability of the left heart and the effect of coronary occlusion. *Circulation Res.* 1976, 38:297-302
- Franklin DL, Citters RLV, Rushmer RF.** Left ventricular function described in physical terms. *Circulation Res.* 1962, 11:702-711
- Kim HC, Min BG.** Factors influencing the peak acceleration of ventricular ejection blood flow in the conscious dog *서울의대 학술지* (Seoul Journal of Medicine) 1983, Vol. 24, No. 2:252-261.
- Levine HF, Bitman NA.** force-velocity relation in the intact dog heart. *J. Clin Invest.* 1964, 43:1383-1396
- Min BG, Fich S, Kostis JB, Doblar D, Kuo PT.** Sensitivity and afterload independence of zero-load aortic flow. *Annals of Biomed. Eng.* 1976, 4:330-342
- Noble MIM, Trenchard D, Guz A.** Left ventricular ejection in conscious dogs: 1. Measurement and significance of the maximum acceleration of blood from the left ventricle. *Circulation Res.* 1966, 19:139-147
- Noble MIM, Stubbs J, Trechard D, Else W, Eisele JH, Guz A.** Left ventricular performance in the conscious dog with chronically denervated heart. *Cardiovasc. Res.* 1972, 6:457-477
- Rushmer RF.** Initial ventricular impulse; A potential key to cardiac evaluation. *Circulation* 1964, 29:268-283
- Sonnenblick EH.** Force velocity relations in mammalian heart muscle. *Am. J. Physiol.* 1962, 202: 931.
- Sonnenblick EH.** Implications of muscle mechanics in the heart, *Fed. Proc.* 1962, 21:975
- Westerhof H, Elzinga G, van den Bos GC.** Influence of central and peripheral changes on the hydraulic input impedance of the systemic arterial tree. *Med. Biol. Eng.* 1973, 11:710-722
- Wilcken DEL, Charlier AA, Hoffman JIE, Guz A.** Effects of alterations in aortic impedance on the performance of the ventricle. *Circulation Res.* 1964, 14:283-293

=국문초록=

대동맥 최대혈류가속도와 좌심실 이완말기 대동맥압간의 관계에 관한 연구

서울대학교 의과대학 의공학교실

민병구 · 김희찬

좌심실의 심근수축을 나타내는 생리변수로서 그 중요성이 주장되어온 “대동맥 최대혈류가속도”에 대해서 등가모델을 이용한 정량적해석 및 의식상태의 5마리의 개에 대한 동물실험을 통한 분석을 실시하였다.

등가모델 해석 결과로 최대혈류가속도가 심근자체의 수축상태뿐 아니라 순환계의 부하상태에 따라서도 변하는 것을 알 수 있었고 동물실험으로 이를 확인하였는바, 대동맥 수축시 최대혈류가속도의 변화치는 1052 ± 431 (cc/sec²) ($p < 0.001$)였고, 이완시는 -1833 ± 799 (cc/sec²) ($p < 0.001$) 이었다.

또한 최대혈류가속도가 좌심실 이완말기의 동맥압에 직접 연관되어있음도 동물실험을 통하여 이들 변화사이의 상관계수가 평균적으로 대동맥 수축시 -0.74 ($p < 0.01$)이었고, 이완시 -0.83 ($p < 0.01$)임을 확인하였다.

본 연구의 결과로, 좌심실 최대 혈류가속도는 순환계 부하상태가 일정한 경우에만 좌심실의 수축상태를 나타내는 생리변수로 사용될 수 있음을 알 수 있었다.